coatings

MDPI

Article

Brazing Temperature Effects on the Microstructure and Mechanical Properties of Ti-45Al-8Nb Joints Using TiZrCuNi Amorphous Interlayer

Sheng Wang [1], Tianle Xu [2], Yingchen Wu [2], Xiguo Chen [1,*] and Xiaohong Yang [2,3,*]

[1] Department of Mechanical Engineering, Quzhou College of Technology, Quzhou 324000, China; wangsheng@qzct.edu.cn
[2] Academician Expert Workstation, Jinhua Polytechnic, Jinhua 321017, China; xtl19841223@163.com (T.X.); 18305724672@163.com (Y.W.)
[3] Key Laboratory of Crop Harvesting Equipment Technology of Zhejiang Province, Jinhua 321017, China
* Correspondence: chenxgvip@qzct.edu.cn (X.C.); 20050626@jhc.edu.cn (X.Y.); Tel.: +86-139-6703-9758 (X.Y.)

Abstract: Ti-45Al-8Nb alloy is widely utilized in the lightweight design of the aerospace field because of its excellent properties. In order to make full use of this alloy, it is important to carry out relevant research, such as into the joining process of Ti-45Al-8Nb alloy. In this work, Ti-45Al-8Nb alloys were successfully connected by a TiZrCuNi amorphous interlayer, which was fabricated using the rapid solidification method. Ti-45Al-8Nb joints were composed of two zones. The typical microstructure of a Ti-45Al-8Nb joint was Ti-45Al-8Nb/AlCuTi + Ti_3Al/(Ti, Zr)(Cu, Ni) + (Ti, $Zr)_2$(Cu, Ni)/Ti_3Al + AlCuTi/Ti-45Al-8Nb. The diffusion of elements between the interlayer and the substrate was enhanced by increasing the brazing temperature, which resulted in an increase in the thickness of the interfacial reaction layer. The maximum shear strength was 171.2 MPa, which was obtained at 930 °C. The typical cleavage fracture was found in all of the Ti-45Al-8Nb joints. The mechanical properties of the joint were compromised at high brazing temperature due to the presence of excessive (Ti, $Zr)_2$(Cu, Ni) phase and coarse Ti_3Al phase, both of which are inherently brittle and harmful to the shear strength of the obtained joint.

Keywords: TiZrCuNi; Ti-45Al-8Nb; brazing temperature; reaction layer; shear strength

Citation: Wang, S.; Xu, T.; Wu, Y.; Chen, X.; Yang, X. Brazing Temperature Effects on the Microstructure and Mechanical Properties of Ti-45Al-8Nb Joints Using TiZrCuNi Amorphous Interlayer. *Coatings* **2024**, *14*, 300. https://doi.org/10.3390/coatings14030300

Academic Editor: Vincent Ji

Received: 31 January 2024
Revised: 23 February 2024
Accepted: 25 February 2024
Published: 29 February 2024

1. Introduction

Currently, heat-resistant steel, Ti-based alloys, Fe-based alloy, and Ni-based alloys are used in the aerospace field, as they possess multiple properties such as hot oxidation and corrosion resistance, and remarkable mechanical properties [1,2]. The properties of these alloys affect engine properties' parameters such as engine thermal efficiency and thrust-to-weight ratio. Generally, developing lightweight and high-temperature-resistant alloys has always been a big concern [3,4]. However, due to drawbacks of these alloys, such as having high density and specific weights, it is difficult for engine parameters to meet requirements. To overcome these disadvantages, TiAl alloy, with its lower density, higher melting point, exceptional strength, and resistance to hot oxidation and creep, has been gradually replacing traditional high-temperature alloys [5–7]. Ti-45Al-8Nb alloy, a type of TiAl alloy, exhibits improved room-temperature plasticity, high-temperature strength, and fracture toughness due to its high Nb content, surpassing that of ordinary TiAl alloys [8–10]. However, achieving practical applications of high Nb-TiAl alloy better, such as fabricating components with complex shapes or large-sized parts, and achieving the application of TiAl alloys in aerospace engine turbine blades, requires solving the problem of connecting high Nb-TiAl alloy with itself and dissimilar materials [11–14].

The joining process for high Nb-TiAl alloys mainly includes fusion welding, diffusion welding, and brazing. Because of the high brittleness of TiAl alloys, cracking easily

occurs after welding thermal cycles, making fusion welding unsuitable for connecting TiAl alloys [15–17]. Diffusion welding involves subjecting the base metal (BM) to high pressure, extended holding time, and elevated temperature, which can lead to transformation of the microstructure and a subsequent reduction in the mechanical properties of the base metal [18]. Moreover, apart from the long thermal cycling time and high cost, diffusion welding cannot effectively connect joints with complex structures [19]. To date, vacuum brazing has the unique advantages of slight joint deformation, no impurity gas pollution, little effect on the mechanical properties of the BM, the capacity to connect complex structures, and the ability to simultaneously connect a host of workpieces, making it an applicable technology for connecting high Nb-TiAl alloys [20,21]. Research by R. K. Shiue et al. [12] shows that using pure Ag filler to weld TiAl alloys led to the brazed seam mainly consisting of Ag-based solid solution, which contains a small quantity of Al and Ti elements. A little bit of Ti_3(Al, Ag) intermetallic compounds are distributed in the brazed seam (BS), resulting in a shear strength of up to 385 MPa. According to the study on pure Ag filler, R. K. Shiue et al. [22] utilized BAg-8 filler for brazing TiAl alloys, leading to the creation of two continuous reaction layers: AlCuTi and $AlCu_2Ti$, attributed to the presence of Ti, Cu, and Ag elements in the BAg-8 filler. The two continuous brittle layers led to a decrease in shear strength to 343 MPa. A study revealed that the Ag-based brazing filler above is suitable for operation below 500 °C, indicating that Ag-based brazing filler cannot meet the requirements of high-temperature applications, and using the precious metal silver inevitably increases costs [23]. Hence, it is worthy and necessary to design and develop appropriate brazing fillers to achieve high-quality connections of TiAl alloys, and amorphous brazing filler has become key due to its strong atomic diffusion ability, excellent wettability, and spreading properties. Although there are already studies on using amorphous filler for brazing high Nb-TiAl alloys, there is still much that needs to be further studied.

Ti-based filler is commonly used in the brazing of TiAl alloys, offering high weld strength. This filler typically consists of Ti-Cu, Ti-Zr-Cu-Ni, and Ti-Zr-Cu-Ni-Co-Mo [21,24]. In this work, the TiZrCuNi amorphous filler was designed and fabricated for brazing the high Nb-TiAl alloy. The interfacial microstructure and formation mechanism of the high Nb-TiAl joints were discussed. The effect of brazing temperature on the microstructure evolution and the shear strength of the joints was evaluated. This work could provide reliable theoretical and experimental data for the lightweight design of the aerospace field.

2. Materials and Methods

Ti-45Al-8Nb used in the experiment were fabricated using an induced skull melting furnace with pure Ti (99.8%), Al (99.99%), Nb (99.9%), which were purchased from Beijing Jinxin Co. Ltd., Beijing, China. The samples for brazing were cut into $4 \times 4 \times 4$ mm^3 and $4 \times 10 \times 10$ mm^3. TiZrNiCu amorphous filler alloy was first melted using the arc melting furnace with chemical composition of 30.21% Ti, 19.76% Zr, 41.83% Cu, 8.19% Ni (wt. %). The alloy ingot was remelted 5 times to become homogenous, and it rapidly solidified in order to obtain the amorphous filler ribbons. The obtained filler ribbon is measured at about 30 μm thick.

Before brazing, the surface of Ti-45Al-8Nb blocks was grounded to 1500 grits using SiC sandpaper. The Ti-45Al-8Nb blocks and TiZrNiCu ribbons are all ultrasonically cleaned in ethanol for 6 min. The TiZrNiCu ribbon was sandwiched between the BM, as shown in in Figure 1a. Then, the assembly samples were placed into the vacuum brazing furnace. The applied temperature was initially raised to 300 °C at a rate of 10 °C/min and held for 30 min before being increased to the target temperature (900, 930, 960, and 990 °C), as illustrated in Figure 2.

The microstructure was examined using the scanning electron microscope (SEM, SU8010, Hitachi, Tokyo, Japan). The phase constitution of the microstrcture was analyzed on the fracture interface using X-ray diffraction (XRD, Bruker D8, Billerica, Germany). A shear strength test of the Ti-45Al-8Nb joints was carried out using the electric universal testing

machine (MTS, CMT4204, Eden Prairie, MN, USA) with a loading rate of 0.5 mm/min, as shown in the schematic diagram (Figure 1b). Three specimens were tested, and the average value of the shear strength was obtained.

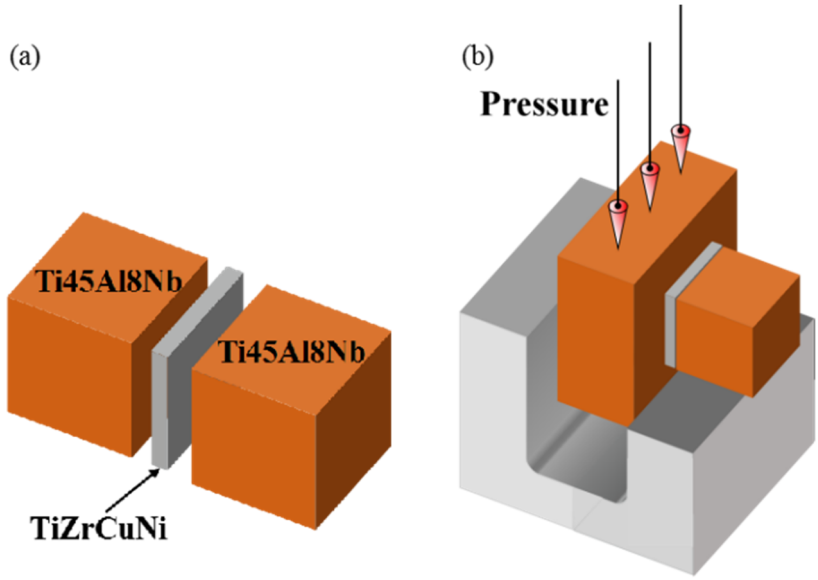

Figure 1. Schematic diagrams: (**a**) assembly samples; (**b**) shear strength test.

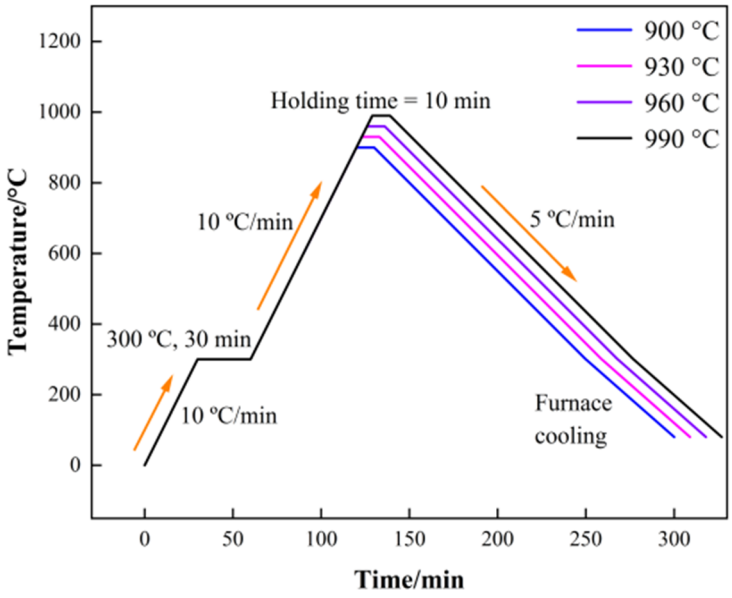

Figure 2. Process curves of brazing.

3. Results and Discussion

3.1. Typical Microstructure of the Ti-45Al-8Nb Joint

The typical microstructure of the joint at 930 °C is shown in Figure 3. No pores and micro-defects can be found in the interfacial microstructure, which demonstrates good metallurgical bonding in the joint. The obtained joint could be divided into two zones: zone I is the brazed seam, and zone II is the reaction layer. The XRD results are depicted in Figure 4, indicating the presence of $(Ti, Zr)_2(Cu, Ni)$, AlCuTi, Ti_3Al, and (Ti, Zr)(Cu, Ni) phases in the joint.

EDS was performed to study the phase formation in the brazed seam. Phase A incorporates 7.04% Al, 12.98% Zr, 1.99% Nb, 28.38% Ti, 10.22% Ni, 39.38% Cu. A previous study [5]

shows that Ti and Zr and Ni and Cu are soluble with each other, in phase A (Ti + Zr): (Cu + Ni) is about 0.83. Combined with XRD results, this phase (phase A) is considered as the (Ti, Zr)(Cu, Ni) phase. Phase B incorporates 2.45% Al, 7.24% Zr, 1.57% Nb, 48.62% Ti, 13.97% Ni, 26.15% Cu, which is $(Ti, Zr)_2(Cu, Ni)$ phase. In phase C and D, Cu:Ti:Al is about 1:1:1. In accordance with the ternary phase diagram of Cu-Ti-Al, it is suggested to be AlCuTi phase. In phase E and F, Ti:Al is about 3:1. In accordance with the ternary phase diagram of Ti-Al, they are suggested to be Ti_3Al phase. Thus, the reaction layer is mainly composed of AlCuTi and Ti_3Al phases, which could be found in previous study [15].

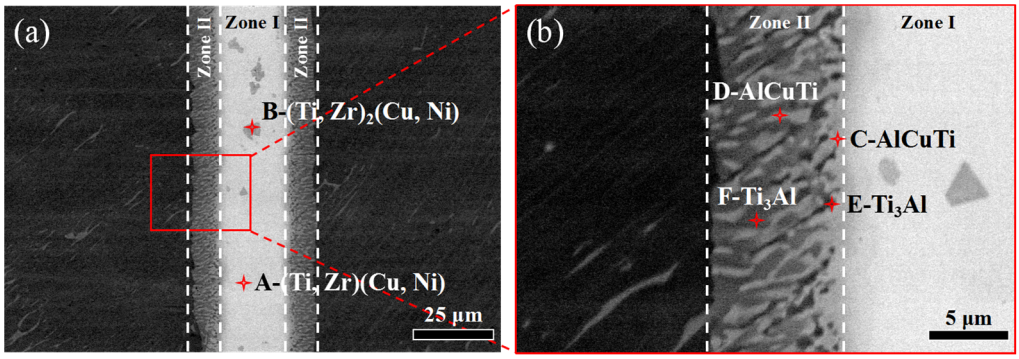

Figure 3. Typical microstructure of Ti-45Al-8Nb joints brazed at 930 °C: (**a**) the brazed seam; (**b**) the reaction layer.

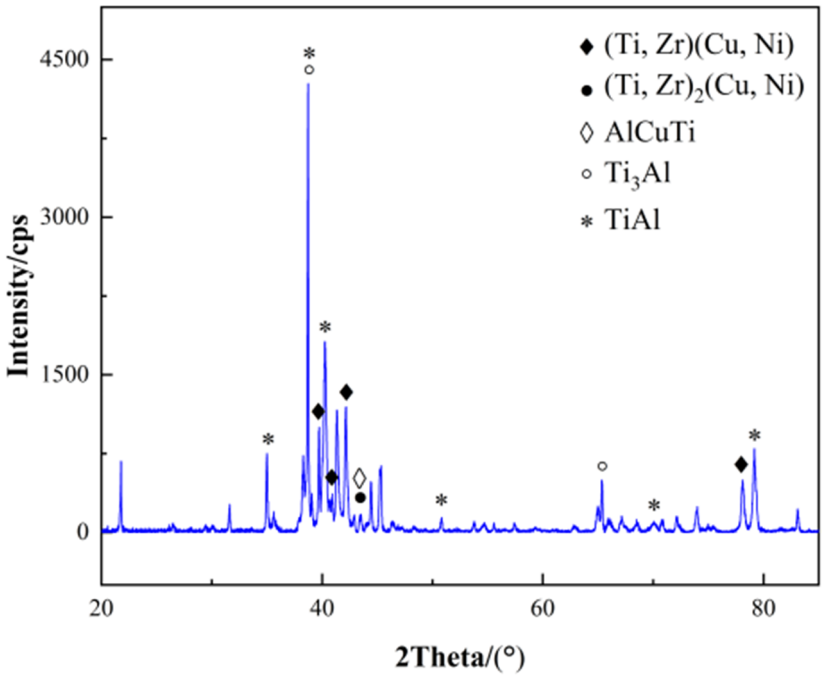

Figure 4. XRD patterns of Ti-45Al-8Nb joints brazed at 930 °C.

To thoroughly analyze the characteristics of the brazed seam, EDS mapping was carried out. It can be seen from Figure 5, Nb can distribute evenly in the brazed seam, which reveals that the element could fully diffuse from the substrate to the brazed seam at 930 °C. The reaction layer mainly consisted of Cu, Al, and Ti elements, and suggested that Ti and Cu have strong affinity. The brazed seam is rich in Ti, Zr, Ni, and Cu, which is similar to the composition of the filler.

The formation mechanism of the typical microstructure can be deduced based on the preceding discussion. During the heating stage, the TiZrNiCu filler effectively wetted the substrate, facilitating the diffusion of Nb, Al, and Ti to the brazed seam. Conversely, Zr,

Cu, and Ni diffused into the substrate. At the interface, Al and Ti would form Ti_3Al phase. During the brazing stage, Cu content would increase at the interface. Based on the Ti-Cu-Al ternary phase diagram [23], the AlCuTi phase can be formed through the reaction formula L + Ti_3Al + TiAl→AlCuTi. At the center of the brazed seam, the primary elements present are Ti, Zr, Ni, and Cu. The eutectic reaction L→(Ti, $Zr)_2$(Cu, Ni) + (Ti, Zr)(Cu, Ni) takes place during the cooling stage.

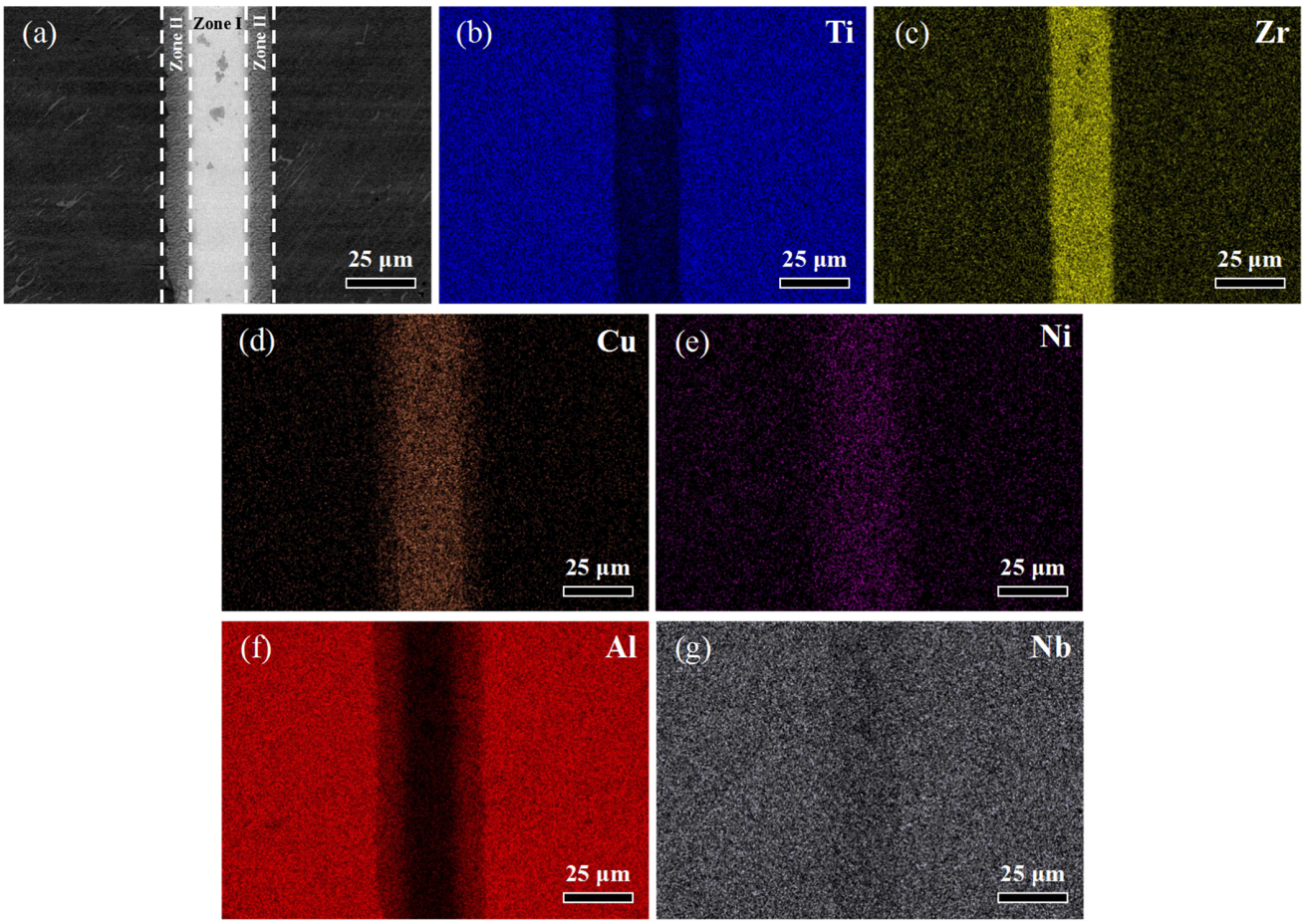

Figure 5. EDS mapping results of Ti-45Al-8Nb joints brazed at 930 °C: (**a**) typical microstructure; (**b**) Ti; (**c**) Zr; (**d**) Cu; (**e**) Ni; (**f**) Al; (**g**) Nb.

3.2. Effect of Brazing Temperature on the Microstructure of Ti-45Al-8Nb Joints

Figure 6 shows the microstructure of Ti-45Al-8Nb joints at various brazing temperatures. The thickness of the brazed seam increases with the duration of the brazing temperature. It could be observed that at 900 °C the reaction layer was about 6.2 μm, and the brazed seam was about 29.4 μm. When the temperature increased to 990 °C, the thickness of the reaction layer and the brazed seam was 13.1 μm and 74.1 μm, respectively.

At 960 °C, the volume fraction of the (Ti, $Zr)_2$(Cu, Ni) phase significantly increased. Furthermore, raising the bonding temperature to 990 °C results in an increase in grain size and the thickness of the brazed seam. White particle phase can be found in (Ti, $Zr)_2$(Cu, Ni) phase. The white phase incorporates 7.01% Al, 10.16% Zr, 1.27% Nb, 37.16%Ti, 7.36% Ni, 37.03% Cu, in accordance with the EDS results (Table 1). (Ti + Zr): (Cu + Ni) is about 1.06, which is (Ti, Zr)(Cu, Ni). It is mainly caused by the increasingly high temperature, which would lead more Zr, Cu, and Ni to diffuse to the substrate and Ti to the brazed seam. The diffusion of elements would cause a shift in the phase diagram towards higher content levels, referring to the phase diagrams (Ti-Ni and Ti-Cu). This facilitates the increase in the (Ti, $Zr)_2$(Cu, Ni) phase, resulting in the presence of more (Ti, $Zr)_2$(Cu, Ni).

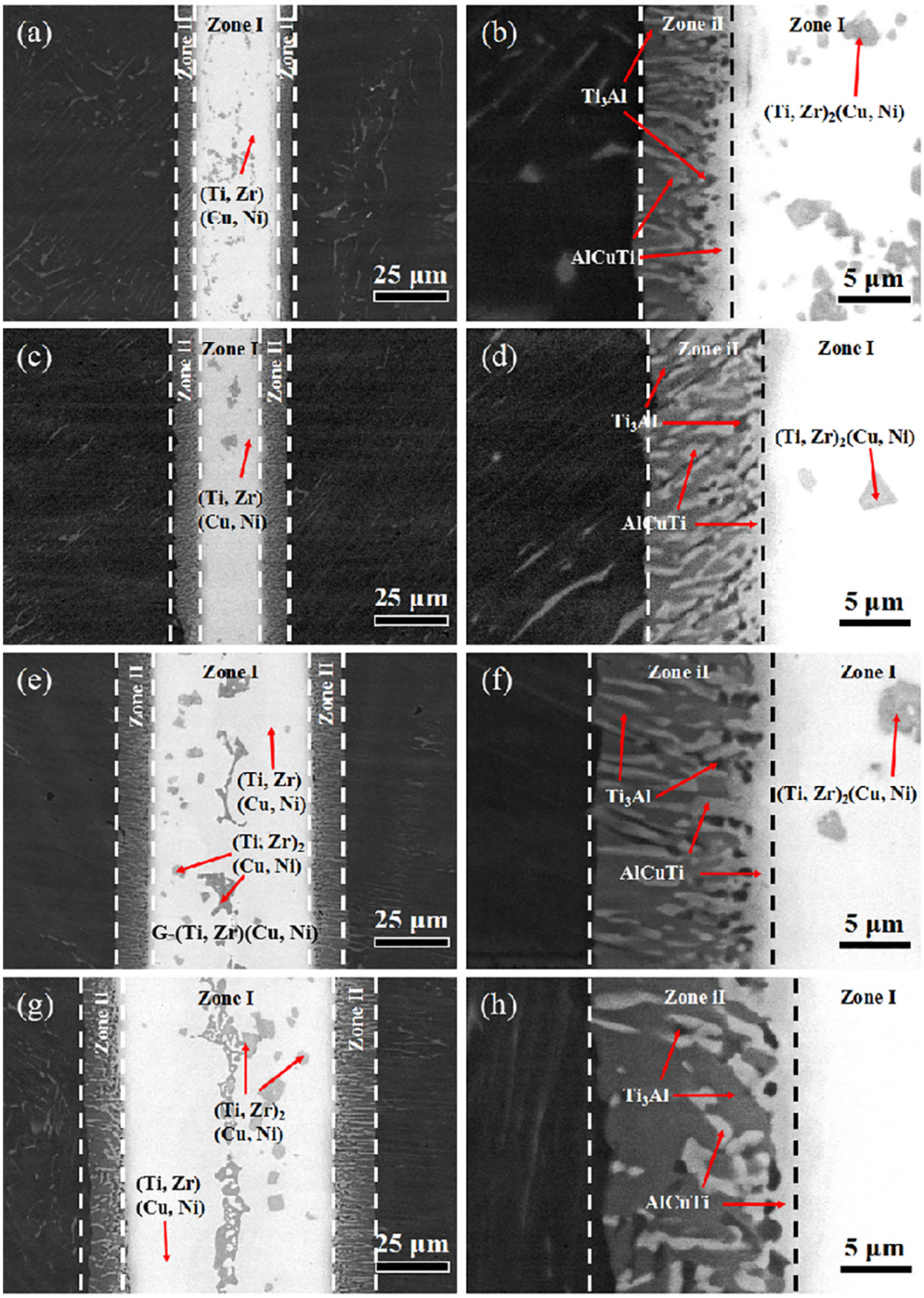

Figure 6. Microstructure of Ti-45Al-8Nb joints at different brazing temperatures: (**a**,**b**) 900 °C; (**c**,**d**) 930 °C; (**e**,**f**) 960 °C; (**g**,**h**) 990 °C.

An appropriate thickness of the Ti_3Al + AlCuTi reaction layer is conducive to obtaining a good brazed joint. When the reaction layer is too thick, the brittle reaction layer is not conducive to relieving residual stress. A thin Ti_3Al + AlCuTi reaction layer is harmful to the shear strength of the Ti-45Al-8Nb joint. Hence, it is necessary to study the growth kinetics of the reaction layer at different processes for obtaining high-quality TiAl alloy brazed joints. Previous studies show that the following equation can be used to calculate the thickness of the reaction layer.

$$x = Dt^{-1/2} \quad (1)$$

$$k = k_0 \exp(-Q/RT) \quad (2)$$

$$\ln k = \ln k_0 - Q/RT \quad (3)$$

where x is the thickness of the reaction layer, D is the diffusion coefficient, t is the dwelling time, k_0 is the diffusion constant, Q is the activation energy, R is the gas constant, and T is the brazing temperature.

Table 1. Chemical compositions and possible phases of each phase in Figures 3 and 6 (in %).

Phase	Al	Zr	Ni	Cu	Ti	Nb	Possible Phase
A	7.04	12.98	10.22	39.38	28.38	1.99	(Ti, Zr)(Cu, Ni)
B	2.45	7.24	13.97	26.15	48.62	1.57	$(Ti, Zr)_2(Cu, Ni)$
C	24.81	4.52	10.42	28.49	26.84	4.93	AlCuTi
D	31.93	2.07	5.96	22.7	32.56	4.78	AlCuTi
E	31.29	1.54	2.20	5.12	52.74	7.12	Ti_3Al
F	25.91	1.48	3.62	9.45	54.41	5.12	Ti_3Al
G	7.01	10.16	7.36	37.03	37.16	1.27	(Ti, Zr)(Cu, Ni)

As shown in Figure 7, the calculated activation energies Q was 185.27 kJ/mol and 341.07 kJ/mol, respectively. Based on these results, the growth kinetics equation of the reaction layer can be inferred, as shown in Equation (4). The growth of the Ti_3Al + AlCuTi reaction layer demonstrates a parabolic trend with the increase in brazing temperature.

$$X_{T\text{-}TiZrCuNi} = 5.05 \times 10^{-3} \exp(-11{,}622.56/T) t^{-1/2} \quad (4)$$

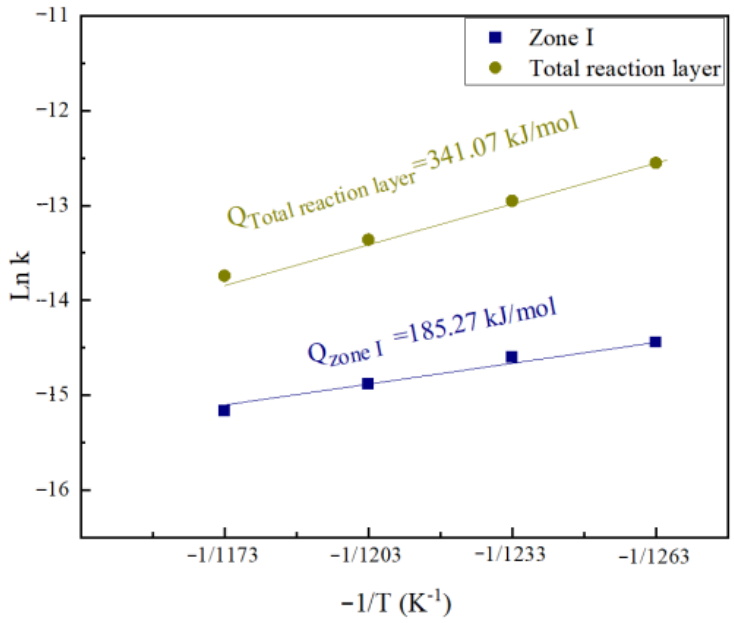

Figure 7. The activation energy pattern.

The mechanical property of Ti-45Al-8Nb alloy brazed joints is closely related to the thickness of the Ti_3Al + AlCuTi reaction layer; the thickness of the reaction layer under different brazing process can be predicted using Equation (5).

$$X_{zone\ I} = 5.05 \times 10^{-3} \exp(-11{,}622.56/T) t^{-1/2} \quad (5)$$

3.3. Effect of Brazing Temperature on the Mechanical Properties of Ti-45Al-8Nb Joints

Figure 8 clearly shows the shear strength of Ti-45Al-8Nb joints brazed at 900, 930, 960, and 990 °C. It is evident from the figure that the overall mechanical performance of the

joints makes good achievement. The shear strength of the joints demonstrates a pattern of initially increasing and then decreasing, as the brazing temperature rises. In the joints brazed at 930 °C, the average shear strength reaches its peak value (171.2 MPa).

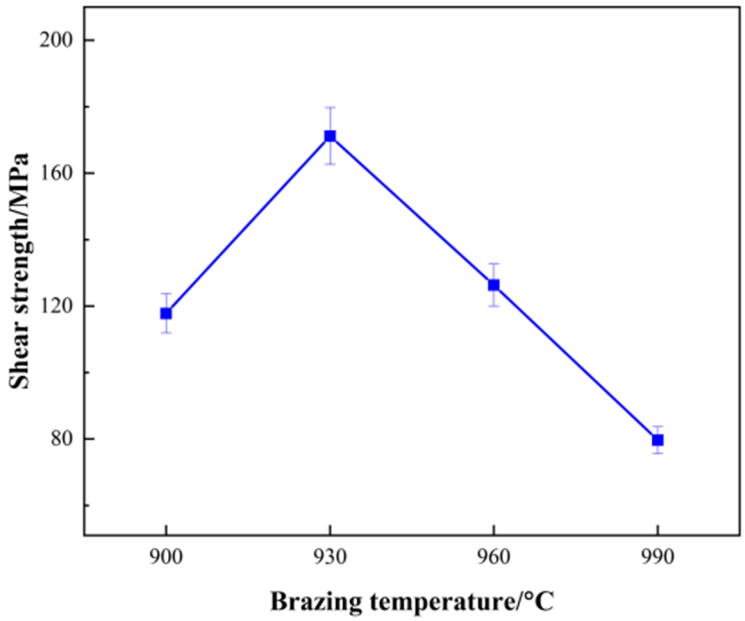

Figure 8. Effect of brazing temperatures on shear strength of Ti-45Al-8Nb joints.

Based on the analysis above, the conclusions could be drawn: as the temperature increases, the mechanical properties remarkably evolved with the evolution of the microstructure of the Ti-45Al-8Nb joint. At 900 °C, the reaction layer is thin, which is not conducive to favorable mechanical properties according to the literature [25]. With the temperature raised to 930 °C, the flowability of the amorphous filler improved, allowing a greater amount of BM elements to dissolve into the molten filler. Consequently, the mutual diffusion of alloy elements such as Ag, Cu, Ti, and Al, and the metallurgical reaction between the BM and the interlayer were more sufficient. The rise in the volume fraction of the phases, such as AlCuTi and Ti_3Al adjacent to the BM, caused the interface reaction layer to become thicker. Previous studies [26,27] have shown that, compared with that of the $(Ti, Zr)_2(Cu, Ni)$ phase, the plasticity of the (Ti, Zr)(Cu, Ni) phase is considerably more superior. The joints at 930 °C presented a moderate reaction layer and the highest volume fraction of the (Ti, Zr)(Cu, Ni) phase, as shown in Figure 6c. In reference [28,29], the Ti_3Al phase exhibits a relatively coarse needle-like morphology at a high temperature. Under the loading process of external force, cracks could occur at this phase, which also decreased the shear strength of the joint at higher temperatures. At 960 and 990 °C, the Ti_3Al phase in the reaction layer increases and displays a relatively coarse needle-like morphology, as depicted in Figure 6e,g. At 960 and 990 °C, the coarsening of grains for brittle intermetallic compounds, such as the Ti_3Al phase, was obviously detrimental to the shear strength. This phenomenon is similar to the previous research [5]: a crack could easily occur in the coarse α_2-Ti_3Al phase under external force. Additionally, the $(Ti, Zr)_2(Cu, Ni)$ phase increased, and under external force, cracks could develop and propagate within this phase, resulting in a decline in the mechanical properties of these Ti-45Al-8Nb joints. Considering these factors, the Ti-45Al-8Nb joint exhibited the highest shear strength at 930 °C.

In Figure 9, the fracture paths and morphologies of joints at various brazing temperatures are shown to delve deeper into the fracture behavior of the joints. It is evident that the fracture mode of the Ti-45Al-8Nb joints was primarily characterized by typical cleavage fractures. As the bonding temperature further increased to 930 °C, the Ti-45Al-8Nb joints predominantly fractured in the center of the brazed seam. It could be deduced that the Ti_3Al + AgCuTi reaction layer could improve the joints' properties to some extent, although

the continuous Ti_3Al layer is inevitably formed [20,21]. At 960 and 990 °C, the fracture path partially shifted to the reaction layer due to the coarsened Ti_3Al phase. In Figure 9e,g, cracks not only went through the reaction layer but also propagated to the BM due to the inherent brittleness of TiAl material and the low connecting strength between the BM and the brittle Ti_3Al phase [24,30,31]. Therefore, it is very necessary and worthy to modify temperature well during the brazing process to obtain a high-quality connection.

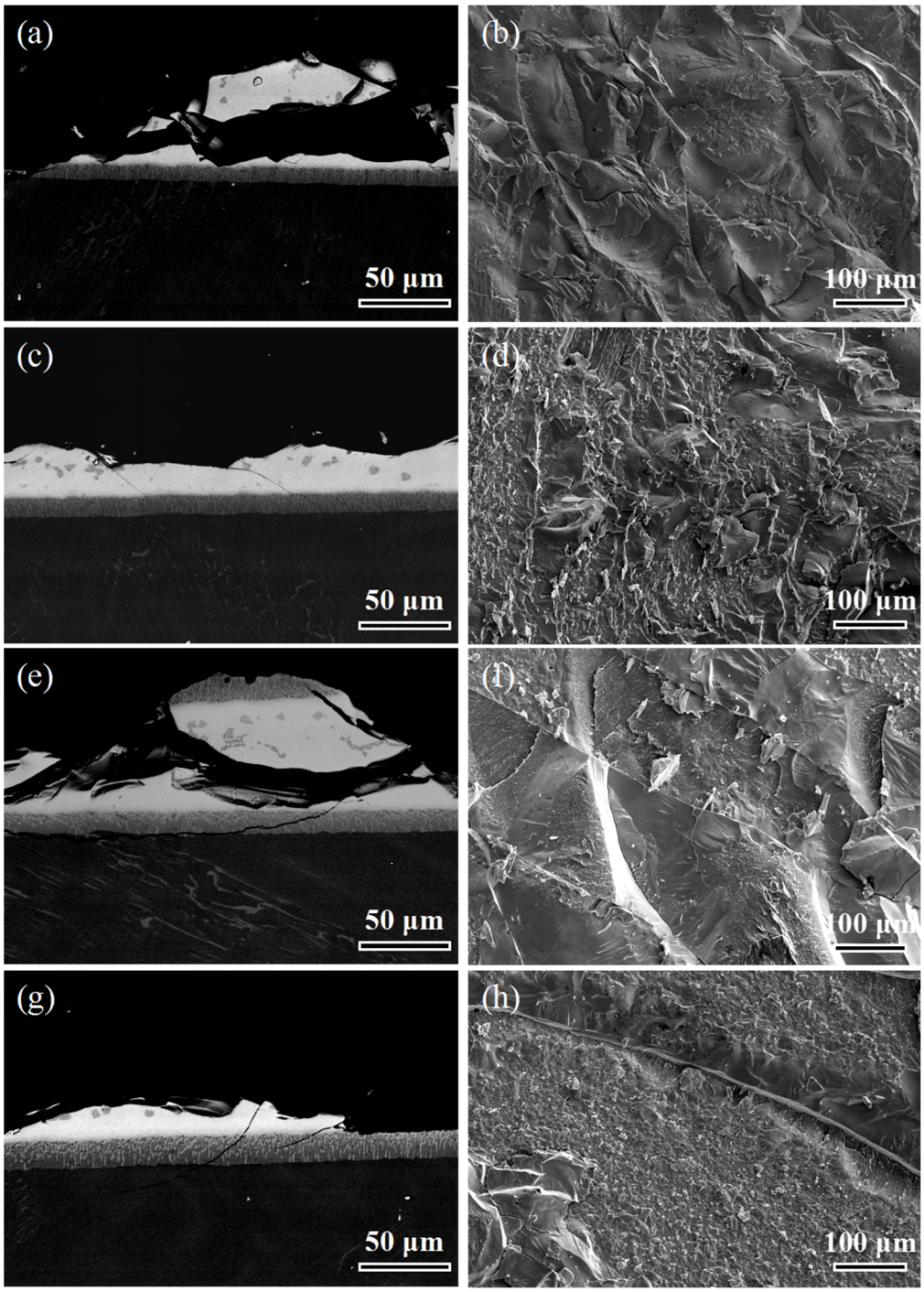

Figure 9. Fracture paths and fracture morphologies of Ti-45Al-8Nb joints at different brazing temperatures: (**a**,**b**) 900 °C; (**c**,**d**) 930 °C; (**e**,**f**) 960 °C; (**g**,**h**) 990 °C.

4. Conclusions

The Ti-45Al-8Nb alloy was connected with the TiZrCuNi amorphous interlayer, and the influence of brazing temperatures on the microstructure and mechanical properties was investigated. The conclusions are given below: The typical microstructure is Ti-45Al-8Nb/Ti_3Al + AlCuTi/(Ti, Zr)$_2$(Cu, Ni) + (Ti, Zr)(Cu, Ni)/Ti_3Al + AlCuTi/Ti-45Al-8Nb. Increasing the bonding temperature facilitated the diffusion of alloy elements and bolstered the metallurgical reactions, resulting in the enlargement of the Ti_3Al phase and the augmentation of the (Ti, Zr)$_2$(Cu, Ni) phase. Additionally, the Ti_3Al + AlCuTi reaction layer thickened with increasing temperature; all the Ti-45Al-8Nb joints demonstrated exceptional mechanical properties. The shear strength of Ti-45Al-8Nb joints peaked at 930 °C (171.2 MPa). Higher bonding temperatures (960 and 990 °C) resulted in a decline in shear strength due to the inherent brittleness of detrimental phases, such as the coarse Ti_3Al phase and excessive (Ti, Zr)$_2$(Cu, Ni) phase. Numerical simulation techniques could provide guidance for future research, such as into the microstructure evolution and stress distribution of the brazed joint.

Author Contributions: Conceptualization, S.W. and X.Y.; methodology, Y.W. and X.C.; formal analysis, X.Y.; investigation, S.W. and X.C.; resources, T.X. and X.C.; data curation, S.W. and X.C.; writing—original draft preparation, S.W. and Y.W.; writing—review and editing, S.W. and X.C. All authors have read and agreed to the published version of the manuscript.

Funding: This work was supported by the National Natural Science Foundation of China [No. 52071165], the Public Welfare Technology Research Project of Zhejiang Province (No. LGC21E050002) and the Science and Technology Plan Project of Quzhou (2023NC07 and 2022NC06).

Institutional Review Board Statement: Not applicable.

Informed Consent Statement: Not applicable.

Data Availability Statement: All data, models, and code generated or used during the study appear in the submitted article.

Conflicts of Interest: The authors declare no conflicts of interest.

References

1. Riedlsperger, F.; Wojcik, T.; Buzolin, R.; Zuderstorfer, G.; Speicher, M.; Sommitsch, C.; Sonderegger, B. Microstructural insights into creep of Ni-based alloy 617 at 700 °C provided by electron microscopy and modelling. *Mater. Charact.* **2023**, *198*, 112720. [CrossRef]
2. Chen, K.J.; Lin, H.M. Effects of niobium carbide additions on Ni-based superalloys: A Study on microstructures and cutting-wear characteristics through plasma-transferred-arc-assisted deposition. *Coatings* **2024**, *14*, 167. [CrossRef]
3. Zhang, W.; Xu, J. Advanced lightweight materials for automobiles: A review. *Mater. Des.* **2022**, *221*, 110994. [CrossRef]
4. Zhang, L.; Long, W.; Du, D.; Fan, Z.; Jiang, C.; Jin, X. A novel diamond/AlSi composite coating on Ti-6Al-4V subStrate made by ultrasonic-assisted brazing. *Coatings* **2023**, *13*, 1596. [CrossRef]
5. Ren, H.S.; Xiong, H.P.; Chen, B.; Pang, S.J.; Chen, B.Q.; Ye, L. Vacuum brazing of Ti_3Al-based alloy to TiAl using TiZrCuNi(Co) fillers. *J. Mater. Process. Technol.* **2015**, *224*, 26–32. [CrossRef]
6. Dong, D.; Xu, H.T.; Zhu, D.D.; Wang, G.; He, Q.; Lin, J.P. Microstructure and mechanical properties of TiC/Ti matrix composites and Ti–48Al–2Cr–2Nb alloy joints brazed with Ti–28Ni eutectic filler alloy. *Arch. Civ. Mech. Eng.* **2019**, *19*, 1259–1267. [CrossRef]
7. Ren, X.Y.; Ren, H.S.; Shang, Y.L.; Xiong, H.P.; Zhang, K.; Zheng, J.H.; Liu, D.; Lin, J.G.; Jiang, J. Microstructure evolution and mechanical properties of Ti_2AlNb/TiAl brazed joint using newly-developed Ti-Ni-Nb-Zr filler alloy. *Prog. Nat. Sci.* **2020**, *30*, 410–416. [CrossRef]
8. Chang, C.; Yang, J. The constitutive equation-based recrystallization mechanism of Ti-6Al-4V alloy during superplastic forming. *Coatings* **2024**, *14*, 122. [CrossRef]
9. Ye, P.H.; Li, X.W.; Wu, H.; Miao, K.S.; Wu, H.; Li, R.G.; Liu, C.L.; Huang, C.X.; Fang, W.B.; Fan, G.H. A bicomponent TiAl alloy with superior compressive strength-ductility synergy prepared by powder metallurgy. *Mater. Sci. Eng. A* **2023**, *884*, 145511. [CrossRef]
10. Zhu, D.D.; Yan, J.F.; Jin, Y.L.; Dong, D.; Wang, X.H.; Ma, T.F. Pressure-induced excellent corrosion resistance of Ti-45Al-8Nb alloy. *Mater. Lett.* **2024**, *355*, 135446. [CrossRef]
11. Cui, S.; Tian, F.; Zhang, S.; Cai, H.; Yu, Y. Numerical simulation and mechanical properties of 6063/6082 dissimilar joints by laser welding. *Coatings* **2023**, *13*, 2049. [CrossRef]
12. Shiue, R.K.; Wu, S.K.; Chen, S.Y. Infrared brazing of TiAl intermetallic using pure silver. *Intermetallics* **2004**, *12*, 929–936. [CrossRef]

13. Cai, X.L.; Li, Q.; Li, H.M.; Xu, G.B.; Yu, H.B. Microstructure evolution and formation mechanism of γ-TiAl/Ni-based superalloy laser-welded joint with Ti/V/Cu filler metals. *Mater. Lett.* **2023**, *333*, 133647. [CrossRef]
14. Cao, H.Y.; Li, H.L.; Wang, D.; Xia, H.B.; Han, K.; Wang, Z.Y.; Zhu, Q.; Liu, D. Dissimilar joining of TC4 and SiC_p/6092Al matrix composite by laser lap welding technology. *Mater. Lett.* **2023**, *351*, 135069. [CrossRef]
15. Dong, D.; Shi, K.Q.; Zhu, D.D.; Liang, Y.F.; Wang, X.H.; Wei, Z.J.; Lin, J.P. Microstructure evolution and mechanical properties of high Nb-TiAl alloy/GH4169 joints brazed using CuTiZrNi amorphous filler alloy. *Intermetallics* **2021**, *139*, 107351. [CrossRef]
16. Wang, Z.W.; Liu, M.; Zhang, H.; Xie, G.M.; Xue, P.; Wu, L.H.; Zhang, Z.; Ni, D.R.; Xiao, B.L.; Ma, Z.Y. Welding behavior of an ultrahigh-strength quenching and partitioning steel by fusion and solid-state welding methods. *J. Mater. Res. Technol.* **2022**, *17*, 1289–1301. [CrossRef]
17. Zhou, J.F.; Zhou, D.W.; Liu, J.S. Effect of oscillating laser beam on the interface and mechanical properties of Ti/Al fusion welding joint. *J. Mater. Res. Technol.* **2022**, *19*, 1993–2007. [CrossRef]
18. Fan, J.F.; Li, X.Q.; Pan, C.L.; Zhu, Z.C.; Wang, X.C.; Qu, S.G.; Yang, C.; Hou, J.B. Microstructure evolution and mechanical properties of pulse high current diffusion bonding γ-TiAl alloy to Ti_2AlNb alloy. *Intermetallics* **2023**, *163*, 108044. [CrossRef]
19. Du, S.G.; Wang, S.L.; Ding, K. A novel method of friction-diffusion welding between TiAl alloy and GH3039 high temperature alloy. *J. Manuf. Process.* **2020**, *56*, 688–696. [CrossRef]
20. Sun, Z.; Zhu, X.X.; Chen, H.Z.; Zhang, L.X. Brazing of TiAl and Ti_2AlNb alloys using high-entropy braze fillers. *Mater. Charact.* **2022**, *186*, 111814. [CrossRef]
21. Song, X.G.; Ben, B.Y.; Hu, S.P.; Feng, J.C.; Tang, D.Y. Vacuum brazing high Nb-containing TiAl alloy to Ti60 alloy using Ti-28Ni eutectic brazing alloy. *J. Alloys Compd.* **2017**, *692*, 485–491. [CrossRef]
22. Shiue, R.K.; Wu, S.K.; Chen, S.Y. Infrared brazing of TiAl intermetallic using BAg-8 braze alloy. *Acta Mater.* **2003**, *51*, 1991–2004. [CrossRef]
23. Li, Y.L.; Liu, W.; Sekulic, D.P.; He, P. Reactive wetting of AgCuTi filler metal on the TiAl-based alloy substrate. *Appl. Surf. Sci.* **2012**, *259*, 343–348. [CrossRef]
24. Zhu, D.D.; Tang, F.H.; Dong, D.; Wang, X.H.; Ma, T.F. Phase formation and nanohardness of Ti-48Al-2Cr-2Nb-1.5C alloy by melt spinning: The effect of cooling rates. *Vacuum* **2024**, *13*, 112985. [CrossRef]
25. Dong, H.G.; Yang, Z.L.; Wang, Z.R.; Deng, D.W.; Dong, C. CuTiNiZrV amorphous alloy foils for vacuum brazing of TiAl alloy to 40Cr steel. *J. Mater. Sci. Technol.* **2015**, *31*, 217–222. [CrossRef]
26. Li, L.; Li, X.Q.; Hu, K.; He, B.L.; Man, H. Brazeability evaluation of Ti-Zr-Cu-Ni-Co-Mo filler for vacuum brazing TiAl-based alloy. *Trans. Nonferrous Met. Soc. China* **2019**, *29*, 754–763. [CrossRef]
27. Feng, G.J.; Wei, Y.; Hu, B.X.; Wang, Y.F.; Deng, D.A.; Yang, X.X. Vacuum diffusion bonding of Ti_2AlNb alloy and TC4 alloy. *Trans. Nonferrous Met. Soc. China* **2021**, *31*, 2677–2686. [CrossRef]
28. Song, X.G.; Cao, J.; Liu, Y.Z.; Feng, J.C. Brazing high Nb containing TiAl alloy using TiNi-Nb eutectic braze alloy. *Intermetallics* **2012**, *22*, 136–141. [CrossRef]
29. Xia, Y.Q.; Dong, H.G.; Hao, X.H.; Li, P.; Li, S. Vacuum brazing of Ti6Al4V alloy to 316L stainless steel using a Ti-Cu-based amorphous filler metal. *J. Mater. Process. Technol.* **2019**, *269*, 35–44. [CrossRef]
30. Galindo-Nava, E.I.; Jing, Y.J.; Jiang, J. Predicting the hardness and solute distribution during brazing of Ti-6Al-4V with TiZrCuNi filler metals. *Mater. Sci. Eng. A* **2018**, *712*, 122–126. [CrossRef]
31. Yuan, L.; Xiong, J.T.; Du, Y.J.; Wang, Y.; Shi, J.M.; Li, J.L. Effects of pure Ti or Zr powder on microstructure and mechanical properties of Ti6Al4V and Ti_2AlNb joints brazed with TiZrCuNi. *Mater. Sci. Eng. A* **2020**, *788*, 139602. [CrossRef]